Sorption and Diffusion of Supercritical Carbon Dioxide into Polysulfone

Muoi Tang,* Yi-Ching Huang, Yan-Ping Chen

Department of Chemical Engineering, National Taiwan University, Taipei, Taiwan, Republic of China

Received 5 September 2003; accepted 26 April 2004
DOI 10.1002/app.20895
Published online in Wiley InterScience (www.interscience.wiley.com).

ABSTRACT: Sorption and diffusion of supercritical carbon dioxide ($SCCO_2$) into polysulfone (PSF) from 313 K and 20 MPa to 333 K and 40 MPa were investigated in this study. A simple gravimetric method was used to measure the mass gain of $SCCO_2$ in PSF, and the Fick's diffusion model was applied to describe the desorption process. The sorption amount, the sorption diffusivity under supercritical states, and the desorption diffusivity at ambient conditions are presented. Comparisons of the sorption amounts and diffusivities of CO_2 for polymers of polycarbonate and PSF are discussed according to the interactions between gas and polymers. The morphology change and plasticization effect attributed to gas sorption in PSF were studied. Effects of glass-transition temperature and yielding stress for PSF and other polymers were used to describe the difference in their diffusivities for the sorption and desorption processes. © 2004 Wiley Periodicals, Inc. J Appl Polym Sci 94: 474–482, 2004

Key words: sorption; desorption; glass transition; diffusion; morphology

INTRODUCTION

Supercritical carbon dioxide ($SCCO_2$), which has low critical properties and desirable chemical safety, is capable as an alternative solvent for polymer processing. Production of polymer foams and dyeing of polymer material[1–3] are examples where swelling and plasticization effects occur after the absorption of $SCCO_2$. The plasticization process accelerates the infusion of additives into polymers and also significantly affects the membrane performance during gas separation.[4] The plasticization effect depends on the sorption amount of $SCCO_2$ as well as its interaction with polymers. Diffusion of $SCCO_2$ into polymers is also influenced by the operating temperature and pressure. Extensive investigations of these phenomena are crucial to further application of $SCCO_2$ in polymer processing.

Various experimental apparatus and methods have been applied to measure the solubility and diffusion kinetics of $SCCO_2$ in polymers. The use of a quartz-crystal microbalance provides an accurate technique,[5] but only equilibrium sorption data were collected. A simple gravimetric method to obtain the diffusion data by measuring the mass gain in polymers was reported in the literature.[6–8] Using this method, the sorption amount was determined by extrapolating the CO_2 weight remaining in the polymer during the desorption process. Gas diffusivities for sorption or desorption at various operating conditions were then evaluated from Fick's law of diffusion.

The sorption and desorption diffusivities of $SCCO_2$ in polysulfone (PSF) were measured in this study using the gravimetric method. A small vessel of 10 mL was used to eliminate possible extrapolation error during the venting period. PSF is usually applied as a gas-separation membrane. The transport properties of CO_2 in PSF have been studied at pressures up to 2 MPa,[9,10] although gas solubility and diffusion data at supercritical conditions are still inadequate. The experimental temperature and pressure were up to 333 K and 40 MPa, respectively, in this study. Diffusivities for $SCCO_2$ in PSF were calculated and compared with our previous study for polycarbonate.[8] The scanning electron microscope (SEM) was used to investigate the morphology change of PSF in the sorption process. Tensile testing and shifting of loss maxima of dynamic mechanical analyses (DMA) were used to characterize the effect of plasticization.

EXPERIMENTAL

Materials

The commercially available polysulfone (PSF, M_n = 26,000) was purchased from Aldrich (Milwaukee, WI). Pellets of PSF were softened at 523 K and pressed

**Present address:* Department of Chemical Engineering, Chinese Culture University, Taipei, Taiwan.
Correspondence to: Y.-P. Chen (ypchen@ntu.edu.tw).
Contract grant sponsor: National Science Council, Republic of China.

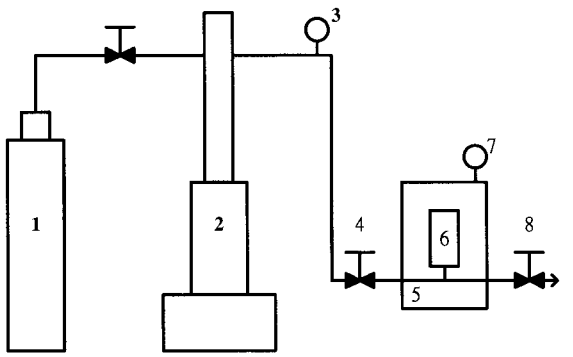

Figure 1 Schematic diagram of the experimental apparatus. 1: CO_2 gas cylinder; 2: high-pressure syringe pump; 3: pressure gauge; 4: check valve; 5: constant-temperature bath; 6: high-pressure cell; 7: temperature indicator; 8: check valve.

to form sheets of 0.8 to 1.2 mm thickness. The sheets were then cut into 40 × 12 mm pieces as the experimental specimens. Carbon dioxide was purchased from San-Fu Chemical (Taiwan) with purity greater than 99.8 mol %.

Apparatus and procedures

A schematic diagram of the experimental apparatus is shown in Figure 1. CO_2 was compressed to the operating pressure by a syringe pump (Model 100DX; Isco, Inc., Lincoln, NE). The weighed specimen was put into a column with a capacity of 10 cm^3. The column was then set in a constant-temperature bath (SFX2-10, Isco). The compressed CO_2 was charged into the column and it took about 10 s to reach the equilibrium pressure. After a desired sorption period, the column was quickly depressurized and the desorption time was recorded. It usually took 40 s before the specimen was immediately taken onto a microbalance (AX105DR; Mettler-Toledo International, Zurich, Switzerland), with sensitivity of 0.01 mg, at room temperature and atmospheric pressure. The weight of the specimen was recorded every 10 s for a period of 150 s. These data were then used to determine the sorption amount and desorption diffusivity of $SCCO_2$ in PSF.

Method of approach

The method for analyzing the data of sorption and desorption was introduced by Berens et al.[6] Fick's law was applied in this study and only diffusion along the thickness direction is analyzed. No edge effect was assumed because the ratio of thickness to length is <0.16. There are two equivalent expressions for the time dependency of mass absorbed in polymer:

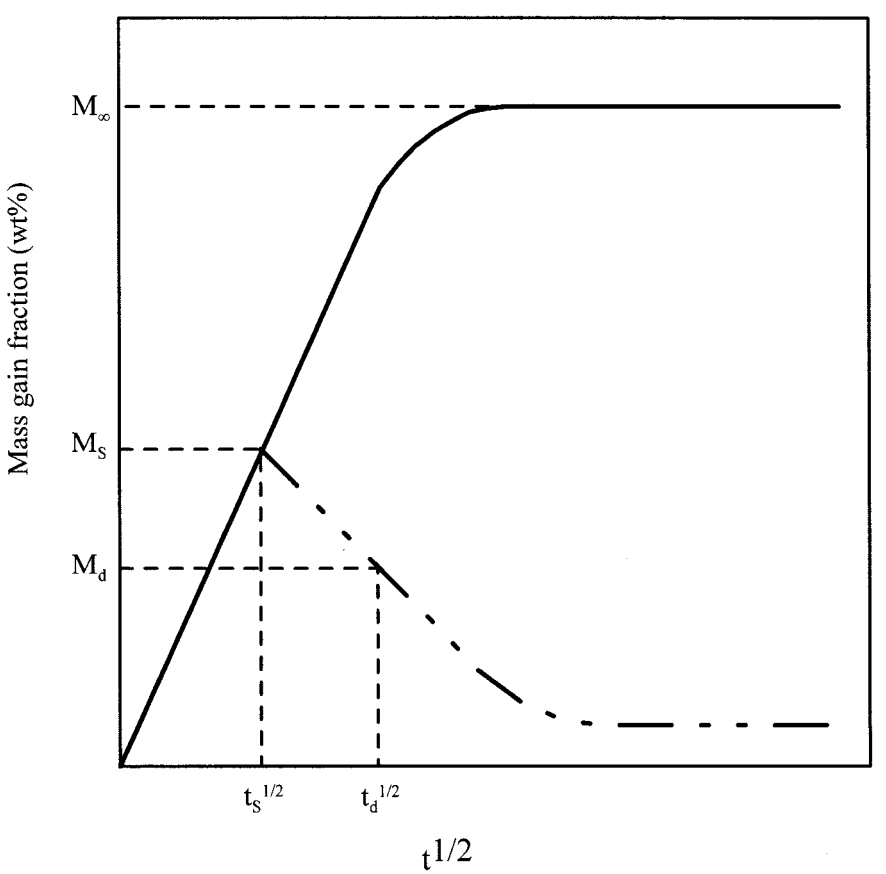

Figure 2 Schematic illustration for the sorption (—) and desorption (— - - — - -) processes. t_s, sorption time; t_d, desorption time; M_∞, saturation amount; M_s, sorption amount at time t_s, M_d, residual amount at time t_d of desorption.

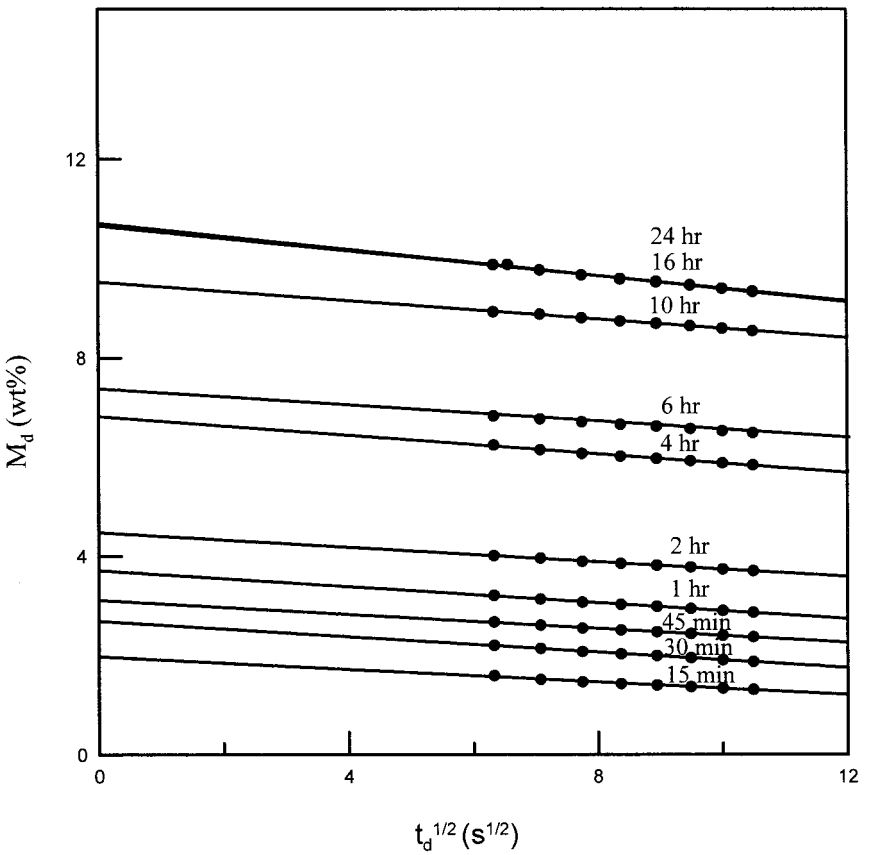

Figure 3 Plot of mass gain (M_d) against the square root of desorption time $(t_d)^{1/2}$ for PSF at 313 K and 20 MPa at various sorption times (t_s).

$$\frac{M_t}{M_\infty} = 4\sqrt{\frac{Dt}{l^2}}\left[\pi^{-1/2} + 2\sum_{n=1}^{\infty}(-1)^n \text{irefc}\left(\frac{nl}{2\sqrt{Dt}}\right)\right] \quad (1)$$

$$\frac{M_t}{M_\infty} = 1 - \sum_{n=0}^{\infty}\frac{8}{(2n+1)^2\pi^2}\exp\left[\frac{-D(2n+1)^2\pi^2 t}{l^2}\right] \quad (2)$$

where D is the constant diffusivity of CO_2, M_t is the amount of sorption during a specific time t_s, and M_∞ is the quantity absorbed after an infinite time period. Both M_t and M_∞ are expressed as the weight percentage of CO_2 per unit weight of the polymer matrix.

The desorption was taken as a short-time process compared to that of sorption. In this case, eq. (1) was simplified by truncating to the first term in the serial:

$$\frac{M_d}{M_s} = -4\sqrt{\frac{D_d t_d}{l^2\pi}} \quad (3)$$

where M_d is the amount that remains in the polymer matrix after desorption time t_d and D_d is the diffusivity for desorption. According to eq. (3), D_d was calculated from the plot of mass gain M_d against $(t_d)^{1/2}$. The sorption amount M_s was obtained by extrapolating to zero desorption time from the desorption mass gain plot.

On the other hand, sorption was taken as a long-time process. With proper estimation of the truncation error, eq. (2) was simplified by truncating to the second term in the serial:

$$\frac{M_s}{M_\infty} = 1 - \frac{8}{\pi^2}\exp\left(\frac{-D_s\pi^2 t_s}{l^2}\right) - \frac{8}{9\pi^2}\exp\left(\frac{-9D_s\pi^2 t_s}{l^2}\right) \quad (4)$$

where t_s is the sorption time and D_s is the diffusivity for sorption. With various M_s values of CO_2 determined at different sorption times, a complete sorption curve was obtained, as illustrated in Figure 2. The D_s parameter was then evaluated from the plot of M_s against t_s/l^2, according to eq. (4).

Characterization

The morphology changes of the polymer specimen were verified using a field emission scanning electron microscope (FESEM; Model 6335F, JEOL, Tokyo, Japan). To analyze the plasticizing effect, the yielding

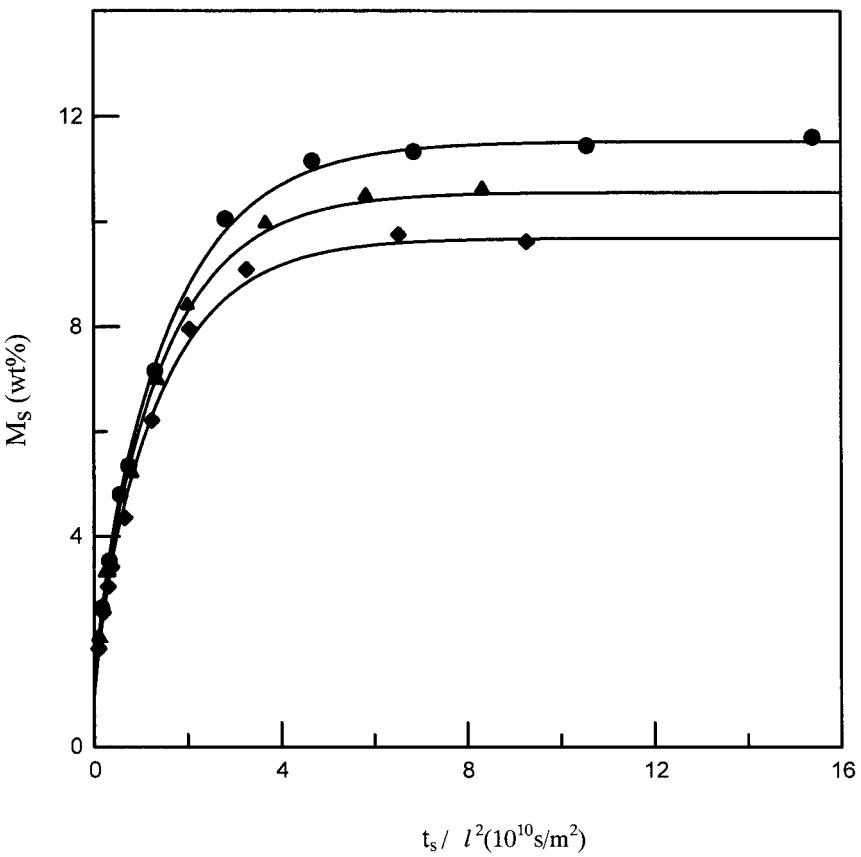

Figure 4 Sorption amounts of PSF at 323 K and various pressures: ◆ 20 MPa, ▲ 30 MPa, ● 40 MPa. Curves are calculated with eq. (8).

stress of the sample was measured using an RTM-1T tensile meter. Dynamic mechanical analyses (DMA; Perkin–Elmer DMA 7e, Norwalk, CT) were used to examine the shifting of loss maxima.

RESULTS AND DISCUSSION

Sorption of CO_2 in PSF

Figure 3 shows a typical plot of the desorption mass gain (M_d) against the square root of the desorption time $(t_d)^{1/2}$ at various sorption times t_s. The linear relationship indicates that Fick's diffusion model is applicable for the experimental data at a short desorption interval. The sorption amounts of $SCCO_2$ (M_s) into PSF were determined by taking the intercepts of the desorption diagram shown in Figure 3. A sorption diagram is then obtained at different t_s periods, as shown in Figure 4. The equilibrium sorption amount (M_∞) in a 40 × 12 × 0.8-mm^3 PSF specimen was reached at around 16 h for all conditions. The CO_2 sorption amounts (M_s) at various sorption times (t_s) were regressed using eq. (4) and the resulting sorption curves are shown in Figure 4. Satisfactory agreement between the experimental and calculated results indicates that the truncated Fick's diffusion model is applicable.

Plots of M_∞ isotherms against pressure are shown in Figure 5. The equilibrium sorption amounts increase with pressure and decrease with temperature, as observed in previous studies of $SCCO_2$ sorption in poly(vinyl chloride)/(PVC) and polycarbonate (PC).[8,12] At higher pressure and lower temperature, it is easier for CO_2 to condense and to be trapped into the polymers. Compared with our previous work,[8] the M_∞ values of CO_2 in PC are higher than those in PSF.

It has been shown in literature that the interaction between CO_2 and the main-chain carbonyl functional group increases the dissolution of CO_2 in PC.[4,6,13] It explains why the CO_2 sorption amount is higher in PC than that in PSF, as depicted in Figure 5. When M_∞ is plotted against CO_2 density, the solubility graph is shown in Figure 6. The CO_2 density is calculated using the Peng–Robinson equation of state[14] at a given temperature and pressure. Generally, the CO_2 solubility increases with density in PSF and PC. A dual-mode model[8,9,13,15] has been suggested for the gas-sorption mechanism is glassy polymers. At a lower density, greater gas solubility is observed at a lower temperature. At a higher density, however, greater gas sorp-

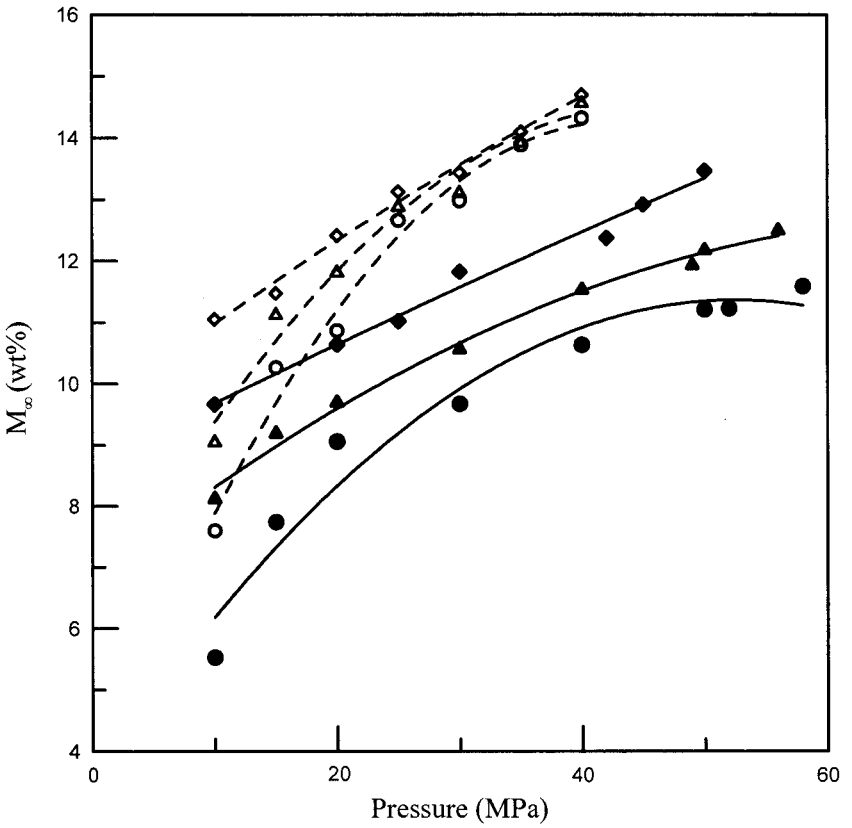

Figure 5 Plot of the equilibrium sorption amount of CO_2 (M_∞) against pressure at various temperatures: ◆, ◇ 313 K; ▲, △ 323 K; ●, ○ 333 K; solid symbols for PSF in this study and open symbols for PC in our previous study.[8]

tion is found at a higher temperature, attributed to the increase in polymer chain mobility to accommodate more CO_2. This behavior was reported in our previous study for PC, as shown in Figure 6, where a crossover point was reached at a density of 680 kg/m^3. The crossover point for PSF polymer substrate was not found in this study. This result can be explained by the difference in glass transition temperatures (T_g) of various polymers. As shown in previous studies, the crossover densities for poly(ethylene terephthalate) (PET) and PC are about 400 and 680 kg/m^3, respectively. The T_g values for various polymers are in the order of PET $<$ PC $<$ PSF. The crossover density for PSF is thus higher than that of PC, and cannot be observed in the operating range of this study.

DESORPTION AND SORPTION DIFFUSIVITIES

From the slopes of the plot of M_d against $(t_d)^{1/2}$, as shown in Figure 3, the diffusivities for desorption (D_d) at ambient temperature and pressure were determined according to eq. (3). Values of D_d at various operating conditions, together with the corresponding CO_2 density and the M_∞ data, are shown in Table I. The plot of D_d against M_∞ for PSF is shown in Figure 7. Desorption diffusivities increase significantly with the CO_2 concentration in the PSF matrix. The largest D_d value is 2.37×10^{-11} m^2/s at 313 K and 40 MPa, corresponding to a maximum CO_2 sorption amount of 12.0 wt % in the PSF substrate. The smallest D_d value is 0.87×10^{-11} m^2/s at 333 K and 20 MPa, where the smallest sorption amount of 9.1 wt % was observed. Comparison of the D_d values for PC[8] and PSF are also presented in Figure 7. Because of the stronger interaction between CO_2 and the carbonyl group of PC, larger CO_2 sorption amounts and smaller D_d values are demonstrated in PC than those in PSF.

The sorption diffusivities D_s were evaluated using eq. (4) with the experimental data shown in Figure 4. The results are also presented in Table I. Figure 8 presents the plot of D_s against temperature at various pressures. It is observed that D_s values for PSF increase with temperature, but are relatively insensitive to pressure. The D_s values for PC were recalculated using our previous experimental data[8] and eq. (4) with truncation to the second-order term. Comparison of D_s for these two polymers, as shown in Figure 8, indicates that higher values are observed for PC. In the sorption process, CO_2 must overcome the polymer chain interaction force to penetrate into the glassy substrate. This force is proportional to the yielding stress of the neat polymer. The yielding stresses for

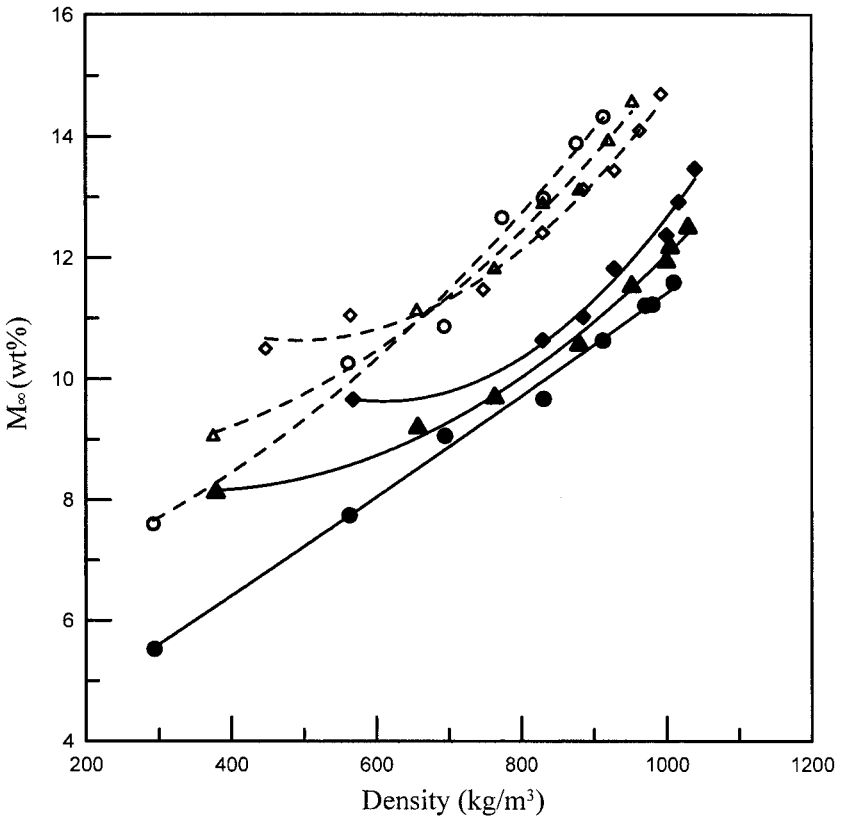

Figure 6 Plot of isotherms for equilibrium sorption amount (M_∞) against CO_2 density: ◆, ◇ 313 K; ▲, △ 323 K; ●, ○ 333 K; solid symbols for PSF in this study and open symbols for PC in our previous study.[8]

neat PC and PSF substrates were measured as 68.1 and 73.0 MPa, respectively. The higher yielding stress of PSF results in a lower D_s value than that in PC. Moreover, the stronger interaction between CO_2 and the carbonyl group of PC is also attributed to the larger D_s data.

The D_d values are larger than D_s values for CO_2 in PSF substrate over the whole range of this study, similar to what we found for the PC substrate.[8] The reason is explained by the plasticization effect for CO_2 in these polymers. On the other hand, Muth et al.[12] showed that $D_s > D_d$ for PVC polymer substrate under $SCCO_2$ conditions. The yielding stress for PVC is 42 MPa. This lower yielding stress favors gas sorption and thus a larger D_s value. The plasticization effect on the diffusivities for PVC is comparatively reduced, although it has a lower T_g value of 360 K.

The plasticization effect on PSF

The CO_2 plasticization effect on PSF was verified by tensile testing and FESEM images in this study. The

TABLE I
Densities of CO_2, Equilibrium Sorption Amount, Desorption Diffusivity, and Sorption Diffusivity at Various Experimental Conditions

Pressure (MPa)	Temperature (K)	Density (kg/m³)	M_∞ (wt %)	D_d (10^{-11} m²/s)	D_s (10^{-11} m²/s)
20	313	830.0	10.6	1.75	0.53
20	323	763.6	9.7	1.22	0.76
20	333	694.9	9.1	0.87	0.88
30	313	927.9	11.8	2.26	0.45
30	323	880.0	10.6	1.78	0.67
30	333	831.2	9.7	1.36	0.89
40	313	991.7	12.0	2.37	0.54
40	323	952.4	11.5	1.90	0.63
40	333	912.7	10.6	1.72	0.95

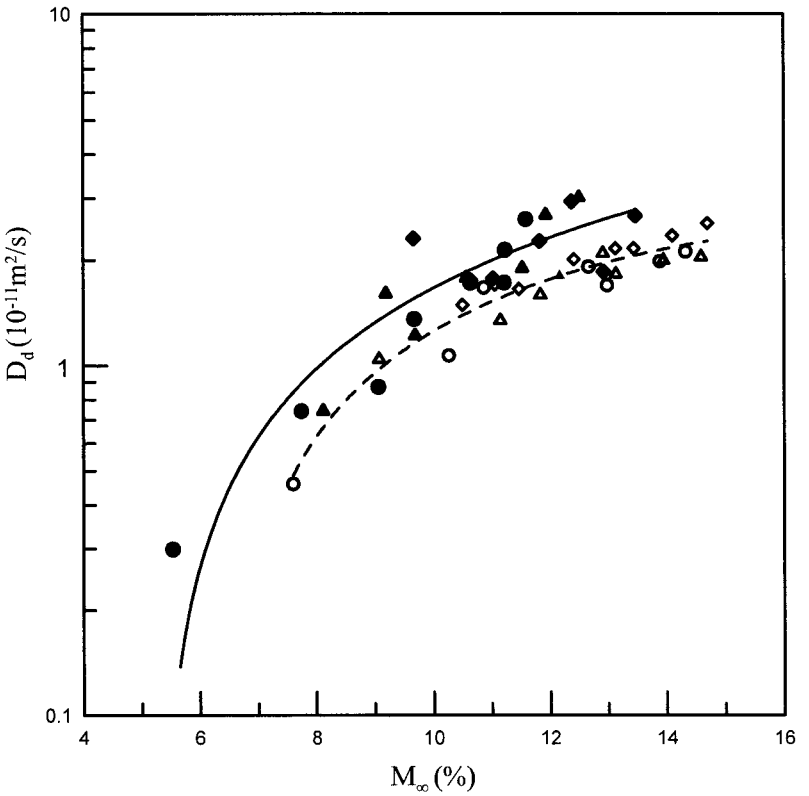

Figure 7 Plot of desorption diffusivity (D_d) against equilibrium CO_2 amount at various temperatures: ◆, ◇ 313 K; ▲, △ 323 K; ●, ○ 333 K; solid symbols for PSF in this study and open symbols for PC in our previous study.[8]

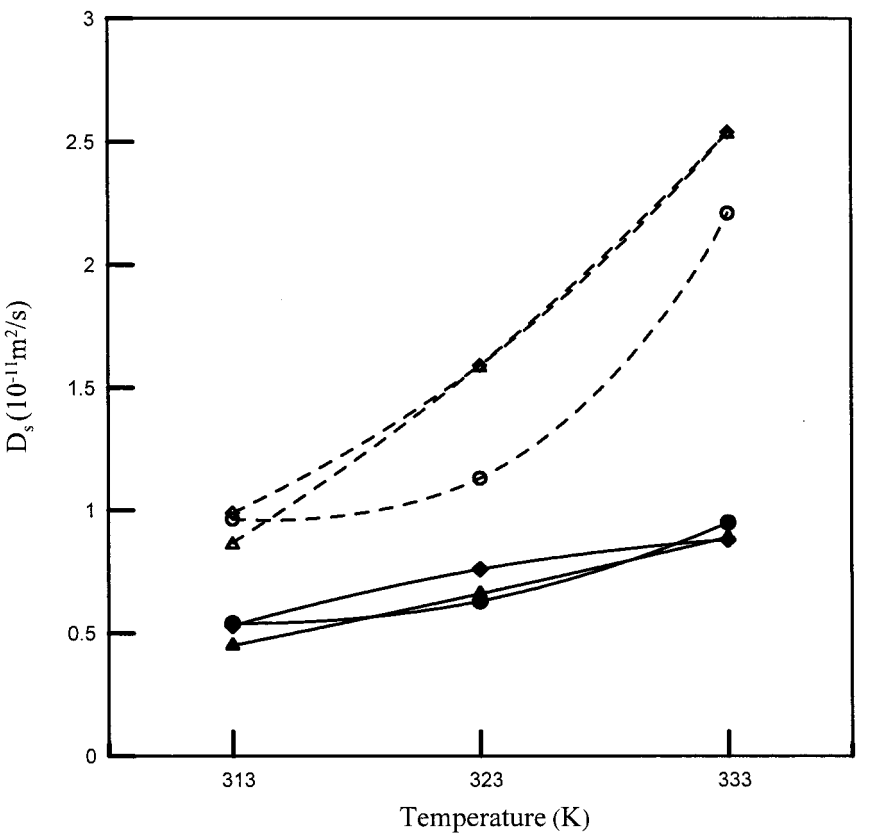

Figure 8 Plot of sorption diffusivity (D_s) against temperature at various pressures: ◆, ◇ 20 MPa; ▲, △ 30 MPa; ●, ○ 40 MPa; solid symbols for PSF in this study and open symbols for PC in our previous study.[8]

TABLE II
Comparison of the Yielding Stress and Mass Gain Fraction for PSF Before and After Being Treated with Supercritical Carbon Dioxide for 24 h

Density (kg/m^3)	Yielding stress (MPa)	Mass gain fraction, M_d (wt %)	
		$t_d = 0$	$t_d = 300$ seconds
Untreated	73.0	—	—
830.0	44.4	10.6	8.5
991.7	35.6	12.0	9.8

PSF sample was treated with CO_2 for 24 h, and the tensile stress was measured at 300 s after venting. The measured data of yielding stress for untreated PSF, the impregnated PSF at two conditions, and the corresponding mass gain fractions are listed in Table II. As shown in Table II, the CO_2 remaining in the sample at a desorption time of 300 s is about 80% of the saturated sorption amount. The PSF sample was plasticized after being treated by CO_2, and the yielding stress decreases with increasing density of CO_2. Its value is about half that of the untreated PSF sample at the highest CO_2 density of 991.7 kg/m^3 (313 K and 40 MPa) in this study. The ×1000 FESEM images at various operating conditions are shown in Figure 9. The defects on the PSF surface resulted from the substrate distortion and the rapid CO_2 depressurization. Compared with the untreated sample in Figure 9(a), no apparent morphology change at lower densities is observed, as shown in Figure 9(b) and (c). At higher densities, shown in Figure 9 (d) and (e), microstructure change and surface deformation arising from plasticization become significant with increasing CO_2 density. Figure 10 presents the loss modulus measured using DMA for PSF treated with CO_2 at various densities, as shown in Figure 9. The treated samples were allowed to remain in ambient conditions for 1 month, where no remaining CO_2 in each sample was assumed. The two loss maxima shown in Figure 10 correspond to two glass-transition states. The plasticization effect is identified by the shifting of loss maxima toward lower temperatures with increasing densities.[16] From our measurements, as shown in Figure 10, the shift of loss maxima from pure PSF to the treated PSF at the highest density (40 MPa and 313 K) are about 4 to 7 K for the two transition temperatures. These results provide further evidence for the plasticization of PSF by $SCCO_2$.

CONCLUSIONS

This study reports the sorption and desorption diffusivities for high-pressure CO_2 in PSF substrate. The

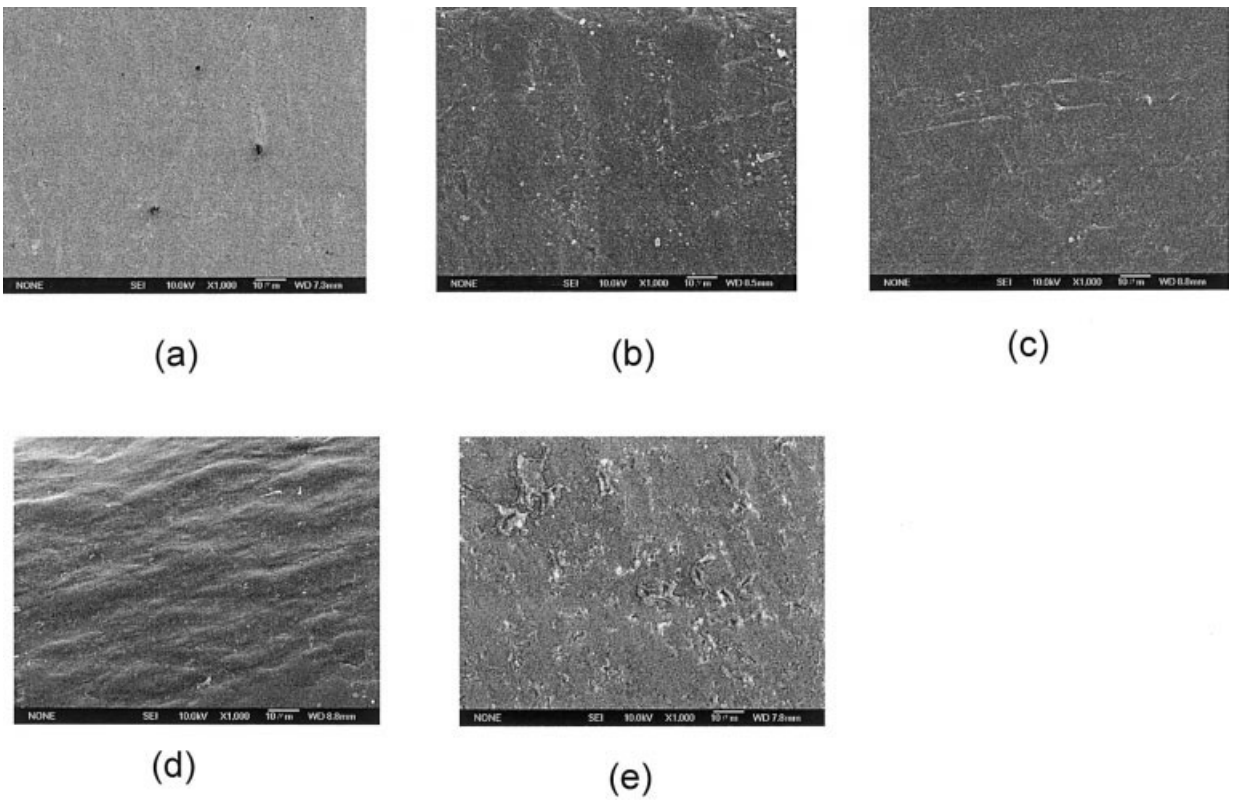

Figure 9 FESEM (×1000) images of polysulfone with $SCCO_2$ at various densities: (a) untreated, (b) 763.6 kg/m^3, (c) 830.0 kg/m^3, (d) 952.4 kg/m^3, (e) 991.7 kg/m^3.

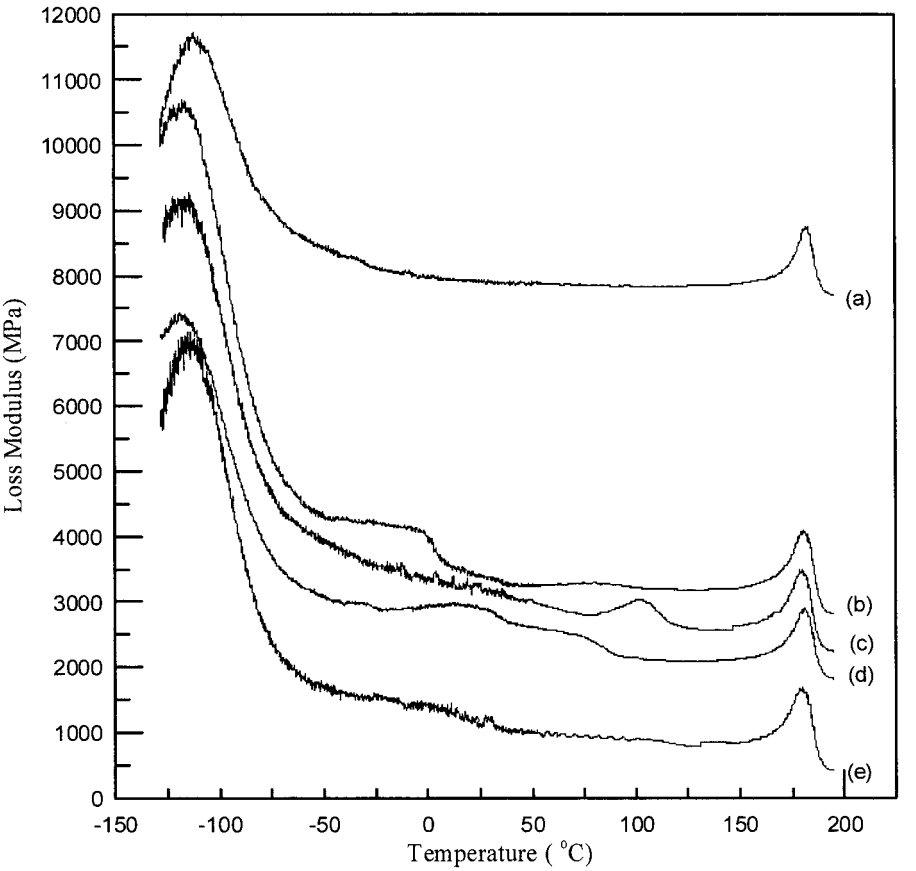

Figure 10 Loss modulus as a function of temperature for polysulfone with $SCCO_2$ at various densities: (a) untreated, (b) 763.6 kg/m^3, (c) 830.0 kg/m^3, (d) 952.4 kg/m^3, (e) 991.7 kg/m^3.

experimental range is from 20 MPa and 313 K to 40 MPa and 333 K. The desorption diffusivity increases with CO_2 solubility. The sorption diffusivity increases with temperature and is insensitive to pressure. Comparison of these measured data with those for PC substrate in our previous study is discussed. The equilibrium sorption amount and sorption diffusivity of CO_2 are lower in PSF than those in PC. The desorption diffusivity, however, is found to be higher in PSF. The plasticization effect for the sorption of CO_2 in PSF is observed in this study from FESEM and yielding-stress measurements, as well as the shifting of loss maxima toward higher $SCCO_2$ densities from DMA measurements for the treated samples.

The authors are grateful to the National Science Council, ROC for supporting this study.

References

1. Krause, B.; Mettinkhof, R.; van der Vegt, N. F. A.; Wessling, M. Macromolecules 2001, 34, 874.
2. Krause, B.; Diekmann, K.; van der Vegt, N. F. A.; Wessling, M. Macromolecules 2002, 35, 1783.
3. von Schnitzler, J.; Eggers, R. J Supercrit Fluids 1999, 16, 81.
4. Bos, A.; Punt, I. G. M.; Wessling, M.; Strahmann, H. J Membr Sci 1999, 155, 67.
5. Aubert, J. H. J Supercrit Fluids 1998, 11, 163.
6. Berens, A. R.; Huvard, G. S.; Korsmeyer, R. W.; Kunig, F. W. J Appl Polym Sci 1992, 46, 231.
7. Webb, K. F.; Teja, A. S. Fluid Phase Equilib 1999, 158–160, 1029.
8. Tang, M.; Du, T. B.; Chen, Y. P. J Supercrit Fluids 2004, 28, 207.
9. Erb, A. J.; Paul, D. R. J Membr Sci 1981, 8, 11.
10. Wang, J. S.; Kamiya, Y. J Membr Sci 1999, 154, 25.
11. Crank, J. The Mathematics of Diffusion, 2nd ed.; Clarendon Press: Oxford, UK, 1975.
12. Muth, O.; Hirth, T.; Vogel, H. J. J Supercrit Fluids 2001, 19, 299.
13. Berens, A. R.; Huvard, G. S. Supercritical Fluid Science and Technology; ACS Symposium Series; American Chemical Society: Washington, DC, 1989; Chapter 14, p. 406.
14. Peng, D. Y.; Robinson, D. B. Ind Eng Chem Fundam 1976, 45, 59.
15. Shieh, Y. T.; Su, J. H.; Manivannan, G.; Lee, P. H. C.; Sawan, S. P.; Spall, W. D. J Appl Polym Sci 1996, 59, 707.
16. Shieh, Y. T.; Liu, K. H. J Supercrit Fluids 2003, 25, 261.